TRENDS IN SCIENCES 2026; 23(6): 12824
https://doi.org/10.48048/tis.2026.12824 RESEARCH ARTICLE

Mechanistic Insights into the Enhancement of Natural Dyeability of PLA Fabrics via Atmospheric DBD Plasma Treatment

Jadsadaporn Chouytan[1], Arisara Suwankosit[1], Suwat Rattanapan[2] and Somchai Udon[1,*]

[1]Division of Textile Technology, Faculty of Textile Industries, Rajamangala University of Technology Krungthep, Bangkok 10120, Thailand
[2]Department of Science, Faculty of Science and Technology, Rajamangala University of Technology Srivijaya, Nakhon Si Thammarat Campus (Sai Yai), Nakhon Si Thammarat 80110, Thailand

([*]Corresponding author's e-mail: somchai.u@mail.rmutk.ac.th)

Received: 27 November 2025, Revised: 15 December 2025, Accepted: 25 December 2025, Published: 10 February 2026

Abstract

Poly(lactic acid) (PLA) is a biodegradable and environmentally sustainable material, although its ability for dyeing is limited, especially with natural dyes. This study examined the application of dielectric barrier discharge (DBD) plasma in atmospheric conditions to enhance the surface features of PLA fabrics without using wetting agents. Experiments utilized the response surface methodology (RSM) analysis for determining the proper condition, including power and plasma exposure time. X-ray photoelectron spectroscopy (XPS) analysis revealed an increase in the O/C ratio from ~0.42 to ~0.59 after 30 s of plasma exposure, while field emission scanning electron microscopy (FE-SEM) images expressed the appearance of nanoscale roughness over the entire fiber surface due to plasma etching. Furthermore, the water uptake increased about 2.5 times, indicating a change in the surface characteristics toward increased hydrophilicity. To analyze the dyeing performance, the Fickian model was used to evaluate the dye diffusion coefficient (D), along with calculating the color strength (K/S). It was found that relatively higher polar dyes like henna and lac exhibited significantly improved dye adhesion, while turmeric and annatto showed only minor changes. The washing fastness results supported this observation; henna and lac maintained stronger color adhesion after treatment, whereas turmeric and annatto showed only modest improvement. Mechanical property tests revealed a slight decrease in yarn strength with prolonged plasma treatment. In conclusion, the pretreatment of PLA fabric with DBD plasma is a clean, chemical-free, and effective method to enhance the dyeing properties of PLA fabric with natural dyes, especially those with relatively higher polarity, if exposure time is controlled within an appropriate range.

Keywords: Poly(lactic acid), Dielectric barrier discharge (DBD) plasma, Surface modification, Natural dyes, Dye diffusion coefficient, Color strength, Washing fastness

Introduction

Poly(lactic acid) (PLA) has been widely studied for textile applications due to its renewable raw materials and biodegradability, while providing mechanical properties that meet the requirements of apparel and technical fabrics [1]. However, PLA fibers have a lower dyeability compared to traditional cellulosic fibers, especially natural dyes. Its backbone consists primarily of aliphatic ester and methyl groups and lacks hydrophilic functional groups (e.g., hydroxyl, carboxyl), which facilitate dye-fiber interactions [2,3]. This low surface energy and hydrophobic character restrict wettability, reduce dye adsorption, and impede the development of stable dye-fiber bonds [4], thus constraining the use of PLA in colored textile products and sustainable dyeing processes. Conventional approaches to improve the dyeability of PLA, such as blending with other polymers [5], surface pre-treatment [6], incorporating functional additives (e.g., organoclay, nanofillers) [7], or optimizing filament cross-section or

crystallinity [8], can be effective but typically require wet chemical reagents, elevated temperatures or prolonged processing, leading to higher water use, effluent generation and potential damage to polymer chains or bulk properties. Consequently, there is strong interest in developing surface-selective, low-impact methods that enhance dye uptake and fastness while retaining the bulk mechanical integrity of PLA. Plasma surface modification has attracted attention as a "dry" and additive-free route to change only the outermost nanometers of a substrate: energetic species in atmospheric or low-pressure plasmas (ions, radicals, metastables, UV photons) can etch surface material, break bonds, and graft oxygen- or nitrogen-containing functionalities [9], producing a more polar and roughened surface that promotes wetting and molecular adhesion without significant bulk modification [10]. A growing body of literature demonstrates that atmospheric plasma approaches, including dielectric barrier discharge (DBD), can increase wettability and improve dye absorption on a variety of textile fibers, making plasma an attractive tool for green textile processing [11-13]. In principle, plasma treatment affects 3 related surface properties that influence dyeability: (i) chemical composition, through the incorporation of oxygen-containing groups (C–O, C=O, O–C=O), which can engage in hydrogen bonding or electrostatic interactions with the dye molecules [14]; (ii) topography, where nanoscale roughness increases the effective surface area and creates adhesion sites [15,16]; and (iii) surface energy, particularly the increase in the polar surface energy component that improves the initial wetting by the dye bath and facilitates the mass transfer of dye molecules to the fiber surface [12]. These modifications are usually evaluated through X-ray photoelectron spectroscopy (XPS), contact angle or water uptake experiments, and scanning electron microscopy (SEM), and several studies have correlated the increased surface oxygen-containing functional groups and raised surface energy to improved dye uptake and intensity [11,17,18]. While plasma treatment generally improves dyeability, the practical implementation requires an optimization of process intensity because excessive exposure can lead to chain scission, over-etching and reductions in mechanical performance and potentially undesirable changes in surface morphology [19,20]. Therefore, an important research question is to identify an operational "window" where surface activation and increased hydrophilicity maximize dye diffusion and fixation, but bulk mechanical degradation is kept within acceptable limits for textile processing and end use. Response surface methodology (RSM) and factorial screening designs have been employed by recent work to map these trade-offs and to derive practical settings for atmospheric DBD plasma treatments [21,22]. Another key aspect is how plasma-induced surface changes translate into kinetics of dye uptake and final color performance for different classes of natural dyes. Among natural dyes, henna (*Lawsonia inermis*) gives a reddish-brown hue and has shown good dyeing performance on a wide range of fibers without the use of heavy-metal mordants [23]. Lac dyes, extracted from *Kerria lacca*, give deep red hues and have recently been reformulated for environmentally friendly dyeing and conditioning of textiles [24]. Turmeric (*Curcuma longa*) gives a bright yellow to orange tone; however, research indicates that its washing fastness is weaker when used without suitable mordants or surface treatment [25]. Annatto (*Bixa orellana*) gives a warm reddish-orange tone and has become recognized as a stable natural dye with high potential for textile applications due to its enhanced color depth and stability when used with bio-mordants [26]. Their different molecular structures and polarities determine how they interact with the modified PLA surface. These molecular differences influence diffusion coefficients under sink conditions, equilibrium sorption (M_∞), color strength (K/S) and washing fastness [27]. Several studies report that dyes with more polar functional groups commonly show higher sensitivity to plasma-activated surfaces, exhibiting larger relative gains in dye uptake and color depth than largely nonpolar dyes [17,28,29]. Systematic diffusion analysis (Fickian modeling) and direct measurement of K/S and CIELAB (L*, a*, b*) coordinates provide the quantitative relation between surface chemistry and macroscopic color performance. However, a clear research gap remains in defining how plasma-induced changes in surface chemistry, nanoscale morphology and hydrophilicity govern dye transport and color development across all dyes of different polarity. Existing studies rarely integrate these surface attributes with dye diffusion behavior, color strength evolution and mechanical consequences under consistent plasma

conditions, leaving the mechanistic basis of plasma-assisted PLA coloration unresolved. In the present work, DBD plasma was applied to PLA fabrics under atmospheric conditions; an RSM pre-screen identified an approximate optimum region and guided the selection of exposure times (0, 10, 20 and 30 s) while fixing plasma power at 150 W to probe the ascent toward the activation peak and avoid over-treatment. Four representative natural dyes (henna, lac, turmeric, and annatto) were selected to sample a range of molecular polarity and size. Surface chemistry was characterized by XPS and correlated with water uptake and FE-SEM examination; dye uptake kinetics were analyzed by short-time Fickian fitting to obtain diffusion coefficients; color strength and CIELAB values were measured by reflectance spectrophotometry and K/S computation; washing fastness was evaluated following ISO 105-C06 with multifiber adjacent fabrics; and tensile testing followed ASTM D2256 protocols to quantify any loss in mechanical performance. By correlating surface characterization with practical dyeing performance, this study aims to (i) determine a plasma exposure window that enhances dyeability, (ii) quantify how dye chemistry mediates sensitivity to surface activation, and (iii) evaluate the compromises between improved coloration and tensile strength. The results are intended to provide actionable guidance for researchers and industry operators attempting more sustainable and efficient methods for producing naturally dyed PLA materials. Compared with earlier studies on DBD plasma-modified PLA fabrics, this work provides an integrated dataset that links oxidation level, nanoscale morphological modification, hydrophilicity, dye molecular structure, diffusion behavior, color development and the associated mechanical response under matched plasma conditions. Guided by a preliminary RSM analysis, the study identifies a practical exposure window and clarifies why dyes with relatively higher polarity show greater sensitivity to plasma functionalization. These results collectively define how controlled plasma activation can enhance coloration while maintaining acceptable mechanical integrity.

Materials and methods

PLA fabric and natural dye sources

PLA multifilament yarns with a linear density of 16.7 tex (150D/64f) were obtained from Ningbo Special Paper Tubes Co., Ltd. (China). The yarns served as both warp and weft in the production of balanced plain-woven fabrics (1/1) with a density of 50 ends per inch (EPI) and 50 picks per inch (PPI) using an automatic weaving machine. Dried leaves of henna tree were obtained from a local community enterprise in Trang Province, Thailand. Lac resin was supplied by Northern Siam Seed Lac Co., Ltd., Lampang Province, Thailand. Dried rhizomes of turmeric were purchased from Asia KGM Co., Ltd., Tak Province, Thailand. Annatto seeds were sourced from a community enterprise in Nan Province, Thailand. All natural dye materials were cleaned, air-dried, and stored in airtight containers at room temperature prior to extraction.

DBD plasma treatment

The surface of the PLA fabric was modified using the DBD plasma system operated at atmospheric conditions. Treatments were carried out with a Mini-Smart plasma generator, PLASMART (Korea), equipped with 2 parallel electrodes and a polyether-ether-ketone (PEEK) dielectric barrier with a discharge gap of 1 mm, as shown in **Figure 1**. The plasma source was driven by a 13.56 MHz RF power supply. The discharge was generated in ambient air, with the relative humidity maintained at approximately 55%. The applied voltage and current were kept stable at 10 kV and 18 mA, respectively. The 10×10 cm^2 of PLA fabric pieces were placed at the center of the discharged zone to ensure uniform exposure. A parametric study varying plasma time (10 - 60 s) and discharge power (50 - 200 W) was carried out under an RSM framework to locate the optimal balance between surface activation and degradation of PLA.

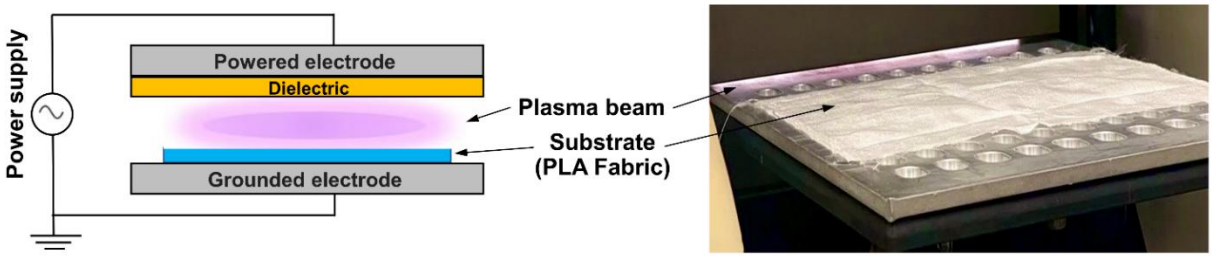

Figure 1 Schematic illustration and actual setup of the DBD plasma treatment applied to PLA fabric.

Experimental design for plasma treatment

A central composite design (CCD) within the framework of RSM was used as a pre-screening stage to determine the operational activation window for atmospheric DBD plasma treatment. The CCD explored plasma exposure time (10 - 60 s) and plasma power (50 - 200 W) over 24 runs, including replicated center points to estimate pure error and enable lack-of-fit testing. This pre-optimization step was performed only to identify the region where hydrophilicity and functional-group formation increased without causing excessive etching.

Table 1 Coded and actual factor levels used in the CCD pre-screen for DBD plasma treatment of PLA fabrics. Axial (±α) levels were chosen to cover the practical operating range of the plasma system.

Factor	Symbol	Coded level (−α)	Coded level (−1)	Coded level (0)	Coded level (+1)	Coded level (+α)
Plasma exposure time	t (s)	10	20	35	50	60
Plasma power	p (W)	50	75	125	175	200

Analysis of the CCD showed that the quadratic model adequately described the relationship between plasma parameters and water uptake (*WU*). Below is the fitted quadratic model used in the analysis:

$$\%\,WU = -1.957 + 0.0624t + 0.0294p - 2.89 \times 10^{-5}tp - 8.36 \times 10^{-4}t^2 - 8.18 \times 10^{-5}p^2$$

The model showed $R^2 = 0.89$ and adjusted $R^2 = 0.86$, with a non-significant lack-of-fit ($p = 0.32$). The coded and actual factor levels are provided in **Table 1**, and a concise ANOVA summary is shown in **Table 2**. Based on the CCD contour plots; an activation region was identified at approximately 150 W and 20 - 30 s.

Table 2 Analysis of variance (ANOVA) for the quadratic response surface model describing the effect of plasma exposure time and power on the water uptake of PLA fabrics. The model was statistically significant ($p < 0.001$), while the lack-of-fit was non-significant ($p = 0.32$), indicating that the quadratic model adequately fits the experimental data.

Source	DF	Sum of squares	Mean square	F value	*p*-value
Model	5	12.84	2.568	18.6	< 0.001*
Residual (pure error)	18	2.48	0.138	-	-
Lack-of-fit	4	0.56	0.140	1.02	0.32 (ns)
Pure error	14	1.92	0.137	-	-
Total	23	15.32	-	-	-

From the contour plots (**Figure 2**), water uptake increased with higher time and power up until reaching an optimum point around 30 s and 150 W. This range likely reflected proper activation, resulting in more polar/rough sites and better wettability. Beyond that window, water uptake decreased. A plausible explanation is over-exposure, chain scission, or surface over-etching can offset polarity gains and make the fibers less hydrophilic [30].

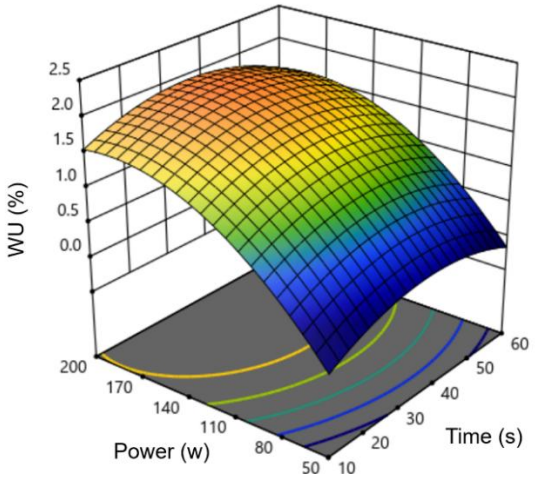

Figure 2 Response surface and contour plots showing the effect of plasma time and power on the water uptake of PLA fabrics.

Based on the response surface results, plasma power was fixed at 150 W, and exposure times of 0, 10, 20, and 30 s were selected to capture the ascending region of the activation curve while avoiding the degradation observed at longer treatments. The CCD optimization served solely to identify this activation window. All mechanistic experiments - XPS, FE-SEM, water uptake, diffusion modeling, color strength evaluation, washing fastness, and tensile testing - were conducted only at these 4 exposure times under the fixed power. These conditions represented the untreated baseline and progressively activated states predicted by the CCD, allowing surface enhancement without excessive fiber damage. The resulting fabrics were subsequently dyed with natural dyes.

Dyeing

Each dye material was cleaned, air-dried, and ground into a fine powder to enhance the extraction efficiency by increasing the surface area. The powdered dyes were extracted with distilled water at a liquor ratio of 1:20. The mixtures were heated at 80 °C for 1 h under gentle stirring. After heating, the extracts were passed through a cotton cloth and then through Whatman No.1 filter paper to remove undissolved solids. To ensure reproducibility among all dye types, the same extraction protocol (raw material mass, temperature, time, and water volume) was applied. Because each natural dye possesses a different inherent hue, the resulting filtrates were then diluted to achieve a consistent visual color intensity appropriate for each dye type under a D65 standard illuminant using a standardized light booth, DCMB 2028, Datacolor (USA). The standardized filtrates were used directly as natural dye solutions for subsequent dyeing. Both untreated and plasma-treated PLA fabrics were dyed using the same dyeing conditions. Dyeing was carried out in a laboratory dyeing machine at a liquor ratio of 1:30, a temperature of 60 °C, and a dyeing time of 30 min, with the pH of the dye bath adjusted to around 6.5 before dyeing. Afterward, the fabrics were rinsed with distilled water to remove surface dye and then dried in an oven at 60 °C until fully dry before testing.

XPS analysis

The effect of plasma exposure at defined exposure times on surface chemistry was analyzed by XPS, PHI VersaProbe 4, ULVAC-PHI (Japan). Measurements were conducted under high vacuum on multiple areas per specimen to check surface homogeneity. High-resolution scans of the C 1 s and O 1 s regions were acquired. The peak components in C 1s were deconvoluted into C–C/C–H, C–O, and O–C=O, and O 1s into C=O and O–C contributions. Relative atomic concentrations and O/C ratios were calculated from the quantified elements.

Surface morphology observation by FE-SEM

Plasma-induced changes in PLA fiber surface, with and without plasma treatment, were examined by FE-SEM using a JSM-IT800SHL, JEOL (Japan). Samples were air-dried, mounted on aluminum stubs

with conductive adhesive, and sputter-coated with gold to form a thin conductive layer. Imaging was carried out at an accelerating voltage of 5.0 kV.

Water uptake measurement

PLA fabrics, both plasma-treated and untreated, were immersed in deionized water under controlled temperature. Dry mass was measured first. Each specimen was vacuum-dried at 50 °C to constant weight, cooled in a desiccator, and weighed to give m_0. For the equilibrium measurement, the specimen was immersed in the test bath until the mass stabilized. At each checkpoint it was withdrawn, blotted with 2 cellulose wipes under a 500 g load for 3 s, and weighed immediately in a draft-shield balance. Equilibrium was defined as 2 consecutive masses taken at least 30 min apart differing by less than 0.1%. The stabilized value was recorded as m_∞. Water uptake at equilibrium (WU_∞) was reported on a dry-mass basis:

$$\%\, WU_\infty = \frac{m_\infty - m_0}{m_0} \times 100$$

Determination of dye diffusion coefficient

The effect of plasma treatment on dyeing was evaluated from dye uptake kinetics. A Fickian model with radial geometry under sink conditions was applied for yielding the diffusion coefficient that used as a quantitative descriptor of the dye-fiber interaction. First step, PLA fabric samples were immersed in dye solutions at 5% on weight of fiber (owf) with a liquor ratio of 1:30 of different natural dyes at 50 °C under gentle agitation. At each time point, the specimen was withdrawn and blotted with 2 layers of cellulose wipes under a 500 g load for 3 s, and weighed immediately in a draft-shield balance to obtain W_t. Immersion continued until the weight stabilized; the equilibrium mass (W_∞) was then recorded. Dry mass (W_0) was determined after vacuum drying at 50 °C. Dye uptake was calculated as:

$$M_t = \frac{W_t - W_0}{W_0}$$

where M_t is the amount of dye absorbed at time,

$$M_\infty = \frac{W_\infty - W_0}{W_0}$$

where M_∞ is the amount of dye absorbed at equilibrium.

In this setting, diffusion is governed by Fick's second law:

$$\frac{\partial C}{\partial t} = D\frac{\partial^2 C}{\partial x^2}$$

where C is concentration of the diffusing species (mol/m^3), t is the elapsed time during the diffusion process (s), x is the position or distance coordinate in the diffusion direction (m), D is the diffusion coefficient.

For a plane sheet of thickness $2L$, assuming uniform initial concentration and constant surface concentration, the fractional uptake can be expressed as described by J. Crank [31]:

$$\frac{M_t}{M_\infty} = 1 - \frac{8}{\pi^2}\sum_{n=0}^{\infty}\frac{1}{(2n+1)^2} exp\left(\frac{(2n+1)^2\pi^2 Dt}{4L^2}\right)$$

where D is the diffusion coefficient (m^2/s) and t is the dyeing time (s).

Following the treatment described by Crank for Fickian diffusion in cylinders, fibers of radius a was used as an effective fabric model, and the analytical solution was fitted to the M_t/M_∞ data. At short times ($M_t/M_\infty < 0.6$), this infinite series can be approximated by its first-term expansion, yielding the short-time approximation [32,33]:

$$\frac{M_t}{M_\infty} = \frac{4}{\sqrt{\pi}}\left(\frac{D}{a^2}\right)^{1/2} \cdot t^{1/2}$$

Then, plotting M_t/M_∞ against $t^{1/2}$ gives a straight line in initial linear region with slope m:

$$m = \frac{4}{\sqrt{\pi}}\left(\frac{D}{a^2}\right)^{1/2}$$

Therefore, the diffusion coefficient (D) can be calculated as equation:

$$D = \left(\frac{m\sqrt{\pi}}{4}\right)^{1/2} . a^2$$

Mechanical testing

The mechanical response was evaluated on yarn specimens rather than woven fabrics to isolate the effect from fabric construction. Tensile testing followed ASTM D2256/D2256M for single-end yarns using a universal testing machine, Autograph AGS-X, Shimadzu (Japan). The gauge length was set to 500 mm and the crosshead speed to 500 mm/min at room temperature. For each treatment level, n = 10 yarns were tested. Tenacity was reported in cN/tex together with elongation at break.

Color measurement

The color depth and appearance of the dyed PLA were quantified by reflectance spectrophotometry. The spectrophotometer, the Color Quest XE, Hunter Lab (USA), was used under illuminant D65 with a 10-degree standard observer. Each specimen was read at a minimum of 5 positions and the mean values were reported. CIELAB coordinates were obtained from the reflectance spectra, where L* denotes lightness, a* locates the red-green axis, and b* the yellow–blue axis. Color strength was expressed by the Kubelka-Munk function, computed from the sample reflectance (*R)* at the wavelength of maximum absorption:

$$K/S = \frac{(1-R)^2}{2R}$$

where *K* represents the absorption component and *S* the scattering component of the dyed substrate.

Fastness testing

Washing fastness was assessed according to ISO 105-C06 A2S using a GyroWash launder-o-meter. Dyed PLA swatches were stitched to a 40×100 mm^2 multifiber adjacent fabric containing acetate, cotton, nylon, polyester, acrylic, and wool. The samples were then placed in stainless-steel canisters together with ten steel balls of 6 mm diameter and a detergent bath prepared with ECE reference detergent at 5 g/L. The liquor ratio was 1:50. Tests were run at 40 °C for 30 min, followed by rinsing with deionized water and air-drying at room temperature. Color change of the PLA and staining on each adjacent fiber were graded on the ISO 1 - 5 gray-scale, where 1 to 5 denote very poor, poor, fair, good, and excellent, respectively.

Results and discussion

Surface chemical changes by XPS analysis

The XPS analysis of the PLA fabrics showed peaks of carbon (C 1s) and oxygen (O 1s) at appreciable amounts. In the C 1s region (**Figures 3(a) - 3(d)**), 3 components were deconvoluted at ~284.8 eV (C–C/C–H), ~286.5 eV (C–O), and ~288.8 eV (O–C=O) [34]. For the untreated fabric, C–C/C–H showed the highest percentage at 44.9%, as shown in **Table 3**, which was consistent with the aliphatic backbone of PLA, whereas C–O and O–C=O were at 31.9% and 23.0%, respectively.

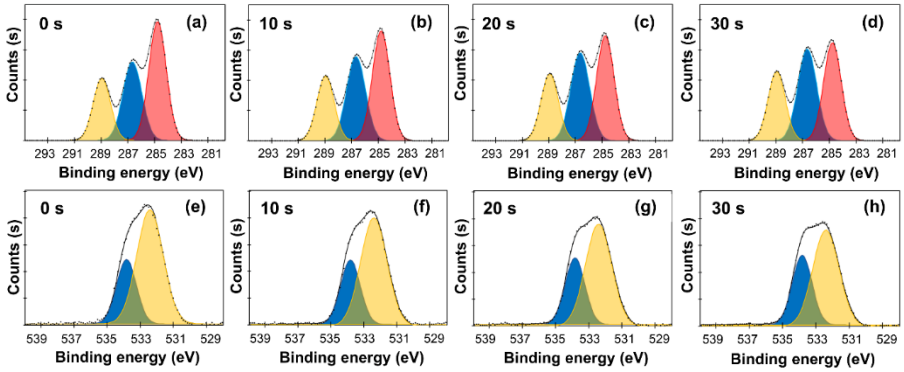

Figure 3 High-resolution XPS spectra of plasma-treated PLA fabrics at different exposure times: C 1s (a-d) and O 1s (e-h) regions. C 1s peaks was deconvoluted into C–C/C–H (red), C–O (blue), O–C=O (yellow). O 1s peaks was resolved into C=O (blue) and O–C (yellow) components.

With plasma exposure for 10 and 20 s, the C–C/C–H peak declined, while the C–O and O–C=O exhibited a noticeable increase, indicating surface oxidation of the fibers [35]. After 30 s, C–C/C–H dropped to about 37.0%. At the same time, C–O and O–C=O rose to 37.3% and 25.7%, respectively. These shifts point to oxygen being grafted onto the surface by plasma oxidation; the gradual increase in C–O and O–C=O also suggests formation of oxygen-containing groups such as hydroxyl and carboxyl that are relevant to surface reactivity [36,37].

Table 3 XPS C 1s and O 1s peak components and O/C ratio of PLA fibers under different plasma exposure times.

Plasma time (s)	C 1s			O 1s		O/C ratio
	C–C (%)	C–O (%)	O–C=O (%)	C=O (%)	O–C (%)	
0	44.96	31.97	23.07	70.34	29.73	0.42
10	41.64	34.29	24.07	69.11	30.96	0.47
20	39.59	35.63	24.78	67.10	32.97	0.51
30	37.03	37.27	25.69	62.52	37.52	0.59

Consistently, the O 1s peak was deconvoluted with 2 main contributions (**Figures 3(e) - 3(h)**), near ~532.4 eV (C=O) and ~533.8 eV (O–C) [38]. Initially, C=O contribution was 70.3%, but it decreased steadily with the plasma treatment, reaching 62.5% at 30 s, in contrast, the O–C fraction grew from 29.7% to 37.5%. This change indicates the formation of hydroxyl groups [39], consistent with the C 1s results. A practical way to view the overall change is the O/C ratio: it rose from ~0.42 for the untreated sample to ~0.59 after 30 s. In simple terms, the surface became more oxygen-rich. Overall, the DBD plasma under atmospheric condition drove a gradual shift from hydrophobic C–C/C–H toward oxygen-containing groups in both the C 1 s and O 1 s spectra. This progressive oxidation represents the surface modification required to enhance the wettability, interfacial adhesion, and dye uptake of PLA fabrics.

Water uptake as a function of plasma time

The water uptake of the PLA fabrics increased noticeably as the plasma exposure time was extended, as shown in **Table 4**, which agrees with the general trend observed from the XPS analysis. For the untreated sample, the water uptake was only about 0.9%, consistent with the naturally hydrophobic surface of PLA dominated by C–C and C–H bonds. After a 10 s plasma treatment, the water uptake rose to roughly 1.6%, and at 20 s it reached around 2.1%. This change corresponds well with the rise in oxygen-containing groups (C–O and O–C=O) detected by XPS. When the treatment time was further increased to 30 s, the growth in water uptake became less distinct, reaching about 2.3%.

Table 4 Water uptake of plasma-treated PLA fabrics at different exposure times.

Plasma time (s)	Water uptake (%)
0	0.93
10	1.57
20	2.05
30	2.28

This suggests that the surface may have approached a limit where additional oxidation no longer produces a strong hydrophilic response. The plateau observed between 20 and 30 s indicated that the surface was nearing saturation in terms of newly formed polar groups, while extended exposure likely introduced early over-etching that partially offset further increases in hydrophilicity. Such opposing effects between activation and surface degradation are commonly reported when plasma treatment approaches its optimal activation threshold. Overall, the higher water uptake values matched the increase in the O/C ratio measured

by XPS (from 0.42 to 0.59). It can therefore be inferred that the plasma treatment enhanced the surface polarity of PLA, making it more receptive to moisture and, consequently, to natural dye molecules during the dyeing process.

Fiber surface morphology

Figure 4 illustrates the FE-SEM series demonstrating the gradual change of the surface of PLA fibers as a result of plasma exposure time. The fiber appeared smooth and compact for the untreated condition (**Figure 4(a)**), showing only a few fine lines along the fiber axis from the spinning process. These features reflected the inherent characteristics of melt-spun PLA, which typically exhibits a uniform surface with minimal defects in the absence of oxidative or etching processes prior to plasma treatment. The initial surface changes were apparent after 10 s (**Figure 4(b)**): the texture became less smooth, while the overall fiber shape remained unaltered. The early surface changes indicated the beginning of surface activation and the establishment of sites that can facilitate dye uptake. At 20 s (**Figure 4(c)**), the surface exhibited a defined etching, featuring a small roughness. These surface features enhanced the effective area and provided more potential binding sites, which can promote the depth of coloration.

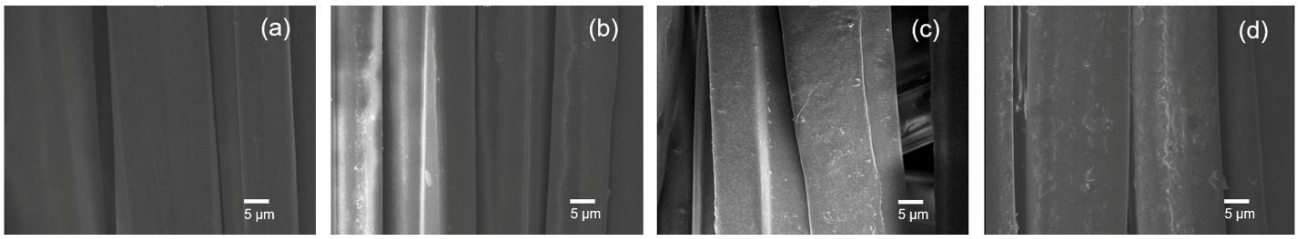

Figure 4 FE-SEM micrographs of PLA fibers after plasma treatments at different exposure times: (a) 0 s, (b) 10 s, (c) 20 s, and (d) 30 s.

With plasma exposure extended to 30 s (**Figure 4(d)**), the surface appeared heavily textured with irregular layers and clear evidence of extensive etching, reflecting pronounced surface alteration. Although this condition offered the highest surface roughness and a greater capacity for dye uptake, it also increased the risk of reduced mechanical stability in the fibers. This interpretation was consistent with tensile testing, which showed reduced tenacity at this stage. Taken together, the images outline a steady progression: longer plasma exposure yielded a rougher, more textured surface. This increase in roughness resulted from continued plasma etching, where prolonged exposure removed more surface material and generated deeper micro-scale features on the fiber. A suitable treatment generally balanced enhanced dyeability with acceptable surface integrity.

Plasma-induced variation in tensile behavior

The tensile results for PLA fibers treated for 0 - 30 are shown in **Figure 5**. With longer plasma exposure, the tensile properties of the yarns declined gradually. The untreated sample showed a tenacity of 4.5 ± 0.8 cN/tex and an elongation at break of 14.2 ± 0.7%, which reflected the inherent strength and ductility of PLA that arose from its semi-crystalline structure and the orientation of polymer chains developed during melt spinning. After 10 s of treatment, both tenacity and elongation dropped slightly, and the reductions became clearer at 20 - 30 s.

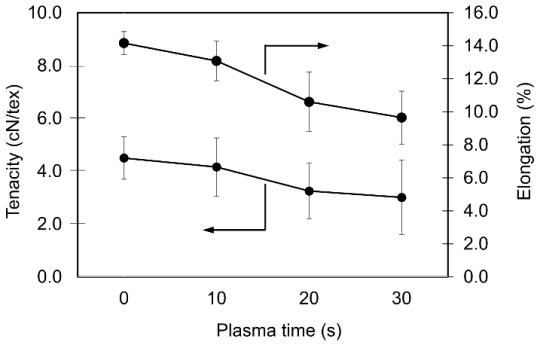

Figure 5 Changes in tenacity and elongation of PLA yarns as a function of plasma treatment time.

The trend was consistent with the FE-SEM observations, where plasma exposure produced surface etching and micro-defects that weaken the fiber structure. In practice, plasma activation improved surface reactivity and dye uptake, but the mechanical performance declined in a steady and modest way, especially beyond 20 - 30 s. Therefore, the treatment time should be tuned to better balance dyeability with the tensile properties needed for processing and end use. Although a measurable decrease in tenacity was observed at 30 s, the remaining strength was still within a range generally considered acceptable for lightweight apparel and other non-load-bearing textile applications. This reduction therefore reflected the expected trade-off between surface activation and mechanical integrity rather than a practical limitation for typical PLA-based textile uses.

Diffusion characteristics of natural dyes

The diffusion of natural dyes into PLA fabrics was markedly influenced by plasma treatment. **Figure 6** illustrates the diffusion profiles of all dyes, which demonstrated a similar pattern. The dye uptake curves rose sharply at the initial stage and then gradually stabilized, approaching equilibrium after approximately 6 h. This trend revealed that the dye transport into the fiber followed the Fickian diffusion law, affected by surface modification. This behavior was consistent with diffusion being governed by the $t^{1/2}$ dependence characteristic of Fickian transport, while plasma-induced increases in surface polarity and roughness facilitated the initial sorption step that controlled the early diffusion rate. **Table 5** shows the diffusion coefficient (D), obtained from the initial slope (< 0.6) of the M_t/M_∞ versus $t^{1/2}$ plots. The linear fitting in this short-time region yielded R^2 values between 0.92 and 0.97 across all dyes and treatment times, confirming that the early uptake behavior was sufficiently linear for reliable estimation of diffusion coefficients.

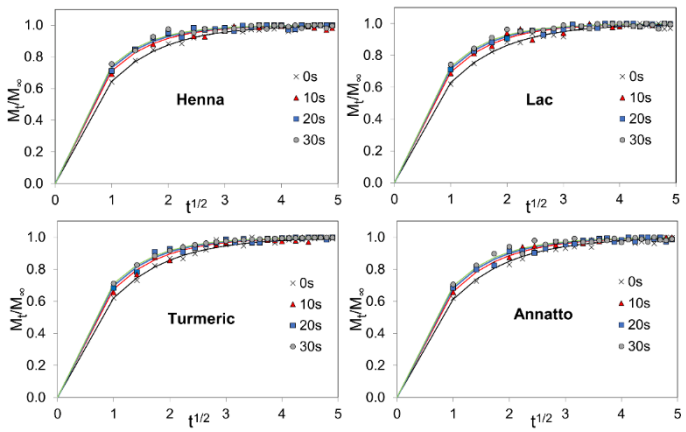

Figure 6 Dye uptake kinetics (M_t/M_∞ versus $t^{1/2}$) of PLA fabrics dyed with henna, lac, turmeric, and annatto under different plasma exposure times.

Table 5 Diffusion coefficients (*D*) of natural dyes in PLA fabrics at different plasma exposure times.

Plasma time (s)	Diffusion coefficients (*D*) (m^2/s)			
	Henna	**Lac**	**Turmeric**	**Annatto**
0	6.80×10^{-10}	6.45×10^{-0}	5.69×10^{-10}	5.32×10^{-10}
10	9.25×10^{-10}	8.58×10^{-10}	7.07×10^{-10}	6.32×10^{-10}
20	1.05×10^{-9}	9.61×10^{-10}	7.82×10^{-10}	7.61×10^{-10}
30	1.13×10^{-9}	1.03×10^{-9}	9.04×10^{-10}	7.99×10^{-10}

The diffusion coefficients increased significantly after 10 s of plasma exposure and increased gradually up to 30 s. Among the examined dyes, henna consistently exhibited the highest diffusion rate, followed by lac, turmeric, and annatto. This was attributed to the relatively small molecular size of lawsone, together with its hydroxyl and carbonyl functional groups, which promoted faster sorption and diffusion into the PLA matrix even before plasma activation. It can be seen that the extent of improvement varied across the dye types, reflecting differences in molecular structure and polarity that strongly influenced their interactions with the modified fiber surface. **Figure 7** shows the electrostatic potential (ESP) maps of all dye molecules visualized using Avogadro software [40] with the electronegativity equalization method (EEM) [41]. The color scale in relative electrostatic potential represents the charge distribution on the molecular surface. These variations indicated the regions likely involved in dye–fiber interactions. Henna, mainly composed of lawsone, contains 1 hydroxyl and 2 carbonyl groups. Before treatment, henna showed the highest diffusivity among the dyes. This behavior was in accordance with these polar functional groups, which readily interacted with activated sites on the PLA surface after plasma treatment, promoting dye uptake. Lac also showed a positive response, which can be attributed to multiple hydroxyl and carboxyl functionalities of laccaic acid, and plasma treatment resulted in a more pronounced increase, with *D* values rising by over 30% between 0 and 10 s of plasma exposure. This suggested that the increase in surface polarity and energy promoted the transport of lac molecules. Turmeric contains several polar groups, such as 2 phenolic hydroxyl and 2 carbonyl groups. These groups are separated by long nonpolar hydrocarbon chains, which decreases their overall polarity. This reduction in polarity occurred because the extended hydrocarbon backbone diluted the contribution of the polar functional groups, limiting their ability to participate in dipole-dipole interactions or hydrogen bonding with the PLA surface. As a result, turmeric exhibited moderate diffusion behavior after treatment compared to henna and lac, with diffusion coefficients increasing by about 24% after 10 s of plasma exposure and showing only minor increases at longer exposure times. In contrast, in annatto, the vast majority of bixin is a long, nonpolar hydrocarbon chain with only 1 carboxyl polar group, which reduces overall polarity and shows the least sensitivity to plasma modification. Its diffusion coefficients increased only about 18% at the 0 - 10 s interval, indicating that its molecular characteristics and steric constraints limited further enhancement despite surface activation. However, because natural dyes are inherently heterogeneous and polydisperse, the diffusion coefficients reported here reflected the overall transport behavior of multiple dye species rather than that of a single molecular entity.

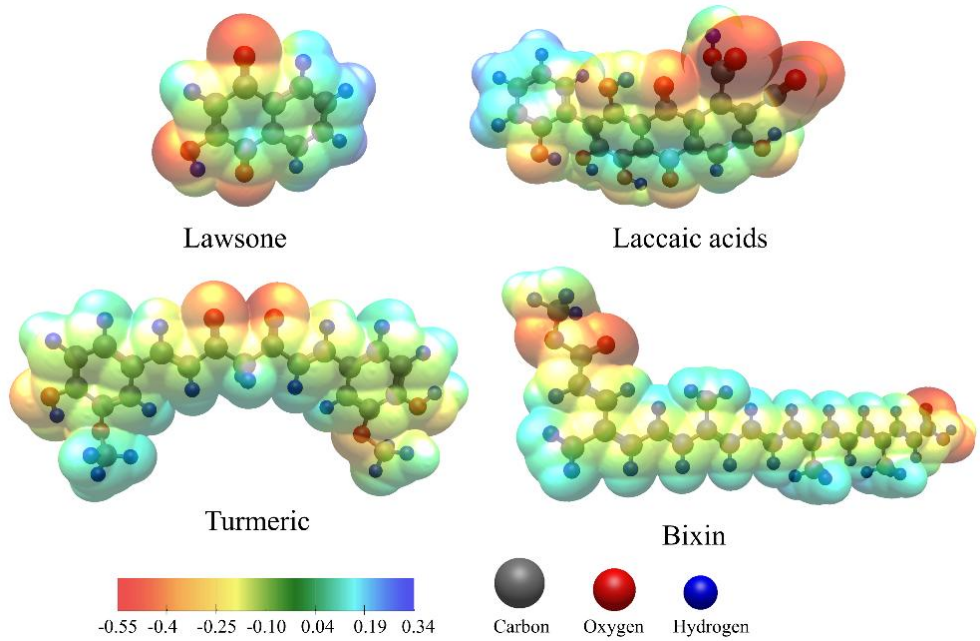

Figure 7 Electrostatic potential (ESP) maps of lawsone, laccaic acids, turmeric, and bixin generated using Avogadro.

These findings confirmed that plasma-induced surface not only improved hydrophilicity but also significantly promoted the dyeability of PLA fabrics with natural dyes, with the most pronounced effect occurring in the first 10 - 20 s of treatment. Such improvement was attributed to the increased surface polarity and nanoscale roughness generated by plasma activation, which facilitated wetting, dye adsorption, and early-stage diffusion into the fiber.

Color strength enhancement

The color strength (K/S) of plasma-treated PLA fabrics dyed with natural dyes significantly increased, and the improvement became more apparent with extended plasma exposure time, as shown in **Table 6**. The untreated PLA fabrics exhibited low dye uptake, as demonstrated by the L*, a*, and b* coordinates, which indicated the fading of the dyed fabrics, as shown in **Figure 8**. This feature was due to the hydrophobic characteristics of PLA and its low reactivity with dye molecules.

Table 6 Color strength (K/S) and CIELAB color coordinates (L, a, b*) of PLA fabrics dyed with natural dyes at different plasma exposure times.

Dyes	Plasma Time (s)	K/S	L*	a*	b*
Henna	0	3.39	71.23	1.38	22.64
	10	5.02	56.27	3.49	36.64
	20	6.52	43.91	3.76	27.22
	30	8.10	32.68	4.96	23.44
Lac	0	2.48	89.21	4.38	10.69
	10	3.12	68.50	17.11	12.91
	20	5.11	56.15	25.65	19.33
	30	6.21	45.26	32.58	22.45
Turmeric	0	2.24	82.59	-5.16	32.62
	10	2.56	78.20	-3.09	46.23
	20	2.98	76.37	4.22	52.10
	30	3.56	68.18	8.41	57.39

Dyes	Plasma Time (s)	K/S	L*	a*	b*
Annatto	0	2.14	74.80	25.21	25.18
	10	2.66	70.71	29.16	34.23
	20	3.05	68.19	31.02	27.12
	30	3.17	59.13	36.41	24.88

However, the use of plasma-treated PLA fabrics for dyeing considerably raised K/S. With a 10 s plasma exposure, K/S showed an initial increase, followed by a more substantial enhancement at 20 s. Fabrics dyed with henna and lac showed a continuous improvement, while those dyed with turmeric and annatto exhibited a slight growth. At 30 s, the increase in color strength diminished, indicating that the surface modification had reached equilibrium. Notably, K/S of the henna and lac on treated fabrics was nearly doubled compared to the untreated fabrics. The pronounced increase was attributed to the relatively higher polarity and the presence of multiple hydrogen-bonding functional groups in both dyes, which interacted more effectively with the oxygen-rich and roughened PLA surface generated by plasma treatment. Nonetheless, the slower increase in K/S between 20 and 30 s was attributed to the saturation of newly formed oxygen-containing functional groups, as supported by the XPS and water-uptake results, together with the onset of mild surface over-etching observed in the FE-SEM images. These competing effects limited further improvements in surface polarity and dye penetration, leading to the observed plateau in color strength.

Figure 8 Color shades of PLA fabrics dyed with natural dyes at different plasma exposure times.

In addition, the color strength measurements were consistent with a shift in the L*, a* and b* coordinates of each color, indicating more saturated shades. Therefore, it could be concluded that DBD plasma treatment directly improved color adhesion on PLA fabrics, attributed to the stronger surface polarity and facilitated transport of dye molecules into the fibers.

Color fastness performance

The fastness testing employed a color fading rating as an indicator for evaluating the dye adhesion performance on PLA fabric after washing, as shown in **Table 7**. In the context of untreated PLA fabrics, all samples faded considerably after washing, with a rating ranging between 1 and 2, or “very poor” to “poor” fastness, which might be attributed to the weak interaction between dyes and the PLA surface. Apparently, henna and lac exhibited slightly better ratings than turmeric and annatto dyes. This difference was attributed to the higher polarity and the greater number of hydrogen-bonding functional groups in henna and lac, which enabled stronger interactions with the oxygen-rich plasma-treated PLA surface and reduced dye desorption during washing.

Table 7 Washing fastness ratings (color change and staining on multifiber adjacent fabrics) of PLA fabrics dyed with natural dyes at 0 s and 30 s plasma treatment.

Dye	Plasma time (s)	Color change	Acetate	Cotton	Nylon	Polyester	Acrylic	Wool
Henna	0	1 - 2	1 - 2	1	1 - 2	1 - 2	1 - 2	1
	30	3 - 4	2 - 3	2	3	3	3	3
Lac	0	1 - 2	1	1	2	1 - 2	1 - 2	1 - 2
	30	3	2 - 3	2	2 - 3	2 - 3	2 - 3	2
Annatto	0	1	1 - 2	1	1 - 2	2	1 - 2	1 - 2
	30	2 - 3	2	1 - 2	2	2 - 3	2	1 - 2
Turmeric	0	1	1	1	2	2	1	2
	30	2 - 3	1 - 2	1 - 2	2 - 3	2	1- 2	2

Nevertheless, when those fabrics were modified by plasma exposure for 30 s, there was an observed enhancement in fastness properties, especially henna, within the range of 3 to 4, or "fair" to "good," reflecting the beneficial polarity of lawsone, which was able to bind with the treated fabrics so that they could not be easily washed off compared to untreated fabric. Meanwhile, the lac-dyed fabric showed a slight improvement in fastness from 2 to 3, or "poor" to "fair," due to the electrostatic attraction between laccaic acid and the modified fabric surface. In the case of turmeric and annatto, they showed only minor increases, which implied that the characteristics of both dye molecules were not responsive to reacting with the PLA fabric even after the plasma treatment, as evidenced by the rating at around 2, or "poor." From the color fastness evaluation on the multifiber adjacent fabrics, there were some differences observed in staining on each component. All dyes exhibited slightly higher staining on natural fibers compared to synthetic fibers, which are inherently less polar. By the way, henna showed a greater stain on wool clearly. Overall, although plasma treatment was unable to sharply enhance color durability, it can be improved to an acceptable level, especially for relatively stronger polar dyes such as henna and lac, which offered an advantage in binding to plasma-treated fabrics.

Conclusions

Experimental results indicate that surface treatment of polylactic acid (PLA) fabrics using dielectric barrier discharge (DBD) plasma is an effective and environmentally friendly method for enhancing the dyeing performance of natural dyes. Plasma treatment introduces oxygen-containing groups onto the fiber surface, which elevates the O/C ratio and enhances the surface hydrophilicity. FE-SEM imaging shows that the fiber surface roughness increases with plasma exposure time, expanding the dye adhesion area. Water uptake results confirm that plasma improves wettability. Such surface treatment results in significant improvements in dyeing qualities, particularly for relatively higher polar dyes such as henna and lac, whose diffusion coefficient and K/S values increase significantly within the first 20 s of plasma exposure time, after which the trend becomes stable. Henna exhibits the most favorable response to the treatment. Lac is the next most effective, while turmeric and annatto have less impact due to their relatively lower polarity and large molecules. Furthermore, washing fastness is significantly improved, especially for fabrics dyed with henna and lac. Plasma treatment enhances the adhesion between the fibers and the dye without the use of chemical mordants. Therefore, the use of DBD plasma is a clean and sustainable approach to enhancing the dyeing performance of PLA fabrics with natural dyes while maintaining the appropriate mechanical strength of the materials.

Acknowledgements

The authors gratefully acknowledge the support and research facilities provided by Rajamangala University of Technology Krungthep, Thailand.

Declaration of generative AI in scientific writing

The authors acknowledge the use of Grammarly and QuillBot solely for improving language clarity and correcting grammar during manuscript preparation. No content generation or data interpretation was performed

by AI. All text was subsequently reviewed and refined by the authors, who take full responsibility for the final content and conclusions.

CRediT author statement

Jadsadaporn Chouytan: Conceptualization; Investigation; Writing - Original Draft; Funding Acquisition. **Arisara Suwankosit**: Resources; Data Curation; Visualization. **Suwat Rattanapan**: Validation; Formal Analysis**. Somchai Udon**: Methodology; Writing - Review & Editing; Project administration.

References

[1] T Hussain, M Tausif and M Ashraf. A review of progress in the dyeing of eco-friendly aliphatic polyester-based polylactic acid fabrics. *Journal of Cleaner Production* 2015; **108**, 476.

[2] R Sutthikitivorakul, P Phinyocheep and W Tessanan. Enhancing mechanical and thermal properties of recycled poly(lactic acid) with multi-branched polyethyleneimine for sustainable recycling applications. *Trends in Sciences* 2025; **22(5)**, 9459.

[3] S Gołębiowska, M Voigt, T Arcos and G Grundmeier. In situ PM-IRRSA and XPS analysis of nitrogen plasma surface modification of polylactide thin films. *Surface and Interface Analysis* 2025; **57(7)**, 499.

[4] G Baig. Coloration of poly(lactic acid) based textiles: A review. *Polimery* 2020; **65(6)**, 415.

[5] N Reddy, D Nama and Y Yang. Polylactic acid/polypropylene polyblend fibers for better resistance to degradation. *Polymer Degradation and Stability* 2008; **93(1)**, 233.

[6] O Avinc and A Khoddami. Overview of poly(lactic acid) (PLA) fibre: part II: Wet processing; pretreatment, dyeing, clearing, finishing, and washing properties of poly(lactic acid) fibres. *Fibre Chemistry* 2010; **42(1)**, 59.

[7] U Tayfun and M Doğan. Improving the dyeability of poly (lactic acid) fiber using organoclay during melt spinning. *Polymer Bulletin* 2016; **73(6)**, 1581.

[8] Z Ju, Y Yang, B Fei and H Hu. Enhancing dyeability of sustainable polylactic acid fabrics through cross-sectional modification of filaments. *Textile Research Journal* 2025; **95(15)**, 1814.

[9] M Bertin, E Leitao, S Bickerton and C Verbeek. A review of polymer surface modification by cold plasmas toward bulk functionalization. *Plasma Processes and Polymers* 2024; **21(5)**, 2300208

[10] S Sakti, P Arinda, T Zafirah, T Putro, N Khusnah and D Santjojo. Morphology and wettability of polystyrene film on QCM sensor caused by oxygen plasma with dc bias. *Trends in Sciences* 2024; **21(11)**, 8318.

[11] T Kim, K Hong, N Thi, and H Manh. The effect of DBD plasma activation time on the dyeability of woven polyester fabric with disperse dye. *Polymers* 2021; **13(9)**, 1434.

[12] S Mowafi, M Taleb and H El-Sayed. A review of plasma-assisted treatments of textiles for eco-friendlier water-less processing. *Egyptian Journal of Chemistry* 2022; **65(5)**, 737.

[13] W Seerlarat, P Porjai, S Phasuk and P Nilsang. Influence of electric potential on dielectric barrier discharge (DBD) cold plasma treatment and its effect on the affinity of leaf printing on cotton fabric. *Trends in Sciences* 2025; **22(11)**, 10461.

[14] J Wang, X Chen, R Reis, Z Chen, N Milne, B Winther-Jensen, L Kong and L Dumée. Plasma modification and synthesis of membrane materials: A mechanistic review. *Membranes* 2018; **8(3)**, 56.

[15] L Phan, S Yoon and M Moon. Plasma-based nanostructuring of polymers: A review. *Polymers* 2017; **9(9)**, 417.

[16] M Fleischer, Z Tuceková, O Galmiz, E Batková, T Plšek, T Kolárová, D Kovácik and J Kelar. Plasma treatment of large-area polymer substrates for the enhanced adhesion of UV-digital printing. *Nanomaterials* 2024; **14(5)**, 426.

[17] V Serrano-Martínez, C Ruzafa-Silvestre, C Hernández-Fernández, E Bañón-Gil, F Arán-Ais and E Orgilés-Calpena. Improving cotton fabric dyeability by oxygen plasma surface activation. *Surfaces* 2024; **7(4)**, 1079.

[18] E Carbone, M Verhoeven, W Keuning and J Mullen. PTFE treatment by remote atmospheric Ar/O_2 plasmas: A simple reaction scheme model proposal. *Journal of Physics: Conference Series* 2016; **715**, 012011.

[19] E Bozacı, K Sever, A Demir, Y Seki, M Sarikanat and E Özdoğan. Effect of the atmospheric plasma treatment parameters on surface and mechanical properties of jute fabric. *Fibers and Polymers* 2009; **10(6)**, 781.

[20] E Bozacı, K Sever, M Sarikanat, Y Seki, A Demir, E Ozdogan and I Tavman. Effects of the atmospheric plasma treatments on surface and mechanical properties of flax fiber and adhesion between fiber-matrix for composite materials. *Composites Part B: Engineering* 2013; **45(1)**, 565.

[21] S Palasakar, R Kale and R Deshmukh. Adhesion properties of DBD plasma-treated nylon 66 fabric - Optimization of plasma process parameters. *International Journal of Adhesion and Adhesives* 2020; **96**, 102446.

[22] S Manjula, O Shanmugasundaram and K Ponappa. Optimization of plasma process parameters for surface modification of bamboo spunlace nonwoven fabric using glow discharge oxygen plasma. *Journal of Industrial Textiles* 2021; **51(2)**, 225.

[23] M Bhuiyan, A Ali, A Islam, M Hannan, S Kabir and M Islam. Coloration of polyester fiber with natural dye henna (*Lawsonia inermis L.)* without using mordant: A new approach towards a cleaner production. *Fashion and Textiles* 2018; **5(1)**, 4069.

[24] J Chouytan, R Thirawat, D Khotradha, T Ruangteprat, I sittitanadol and S Udon. Enhancing the efficiency of hemp fiber dyeing with natural dyes: Indigo and lac. *Journal of Metals, Materials and Minerals* 2024; **34(2)**, 1873

[25] D Hosen, F Rabbi, A Raihan and A Mamun. Effect of turmeric dye and biomordants on knitted cotton fabric coloration: A promising alternative to metallic mordanting. *Cleaner Engineering and Technology* 2021; **3**, 100124.

[26] P Naidis, S Lykidou, M Mischopoulou, E Vouvoudi and N Nikolaidis. Study of the dyeing properties of annatto and ultrafiltrated annatto as colourants for natural fibres. *Journal of Natural Fibers* 2021; **19(14)**, 7885-7895.

[27] S Umbreen, S Ali, T Hussain, T Hussain and R Nawaz. Dyeing properties of natural dyes extracted from turmeric and their comparison with reactive dyeing. *Research Journal of Textile and Apparel* 2008; **12(4)**, 1-11.

[28] A Haji and M Naebe. Cleaner dyeing of textiles using plasma treatment and natural dyes: A review. *Journal of Cleaner Production* 2020; **265**, 121866.

[29] M Naebe, P Cookson, J Rippon, R Brady, X Wang, N Brack and G Riessen. Effects of plasma treatment of wool on the uptake of sulfonated dyes with different hydrophobic properties. *Textile Research Journal* 2010; **80(4)**, 312.

[30] G Primc. Hydrophilization of polypropylene by gaseous plasma treatments and hydrophobic recovery. *Polymers* 2025; **17(19)**, 2644.

[31] J Crank. *The mathematics of diffusion*. 2nd ed. Oxford University Press, London, 1975, p. 44-68.

[32] N Jiang, Y Li, Y Li, T Yu, Y Li, D Li, J Xu, C Wang and Y Shi. Effect of short jute fibers on the hydrolytic degradation behavior of poly(lactic acid). *Polymer Degradation and Stability* 2020; **178**, 109198.

[33] M Azka, S Sapuan, H Abral, E Zainudin and F Aziz. An examination of recent research of water absorption behavior of natural fiber reinforced polylactic acid (PLA) composites: A review. I*nternational Journal of Biological Macromolecules* 2024; **268**, 131845.

[34] A Jorda-Vilaplana, V Fombuena, D Garcia-Garcia, M Samper and L Sanchez-Nacher. Surface modification of polylactic acid (PLA) by air atmospheric plasma treatment. *European Polymer Journal* 2014; **58**, 23-33.

[35] O Laput, I Vasenina, MC Salvadori, K Savkin, D Zuza and I Kurzina. Low-temperature plasma treatment of polylactic acid and PLA/HA composite material. *Journal of Materials Science* 2019; **54**, 11726-11738.

[36] Y Ren, L Xu, C Wang, X Wang, Z Ding and Y Chen. Effect of dielectric barrier discharge treatment on surface nanostructure and wettability of polylactic acid (PLA) nonwoven fabrics. *Applied Surface Science* 2017; **426**, 612-621.

[37] B Hergelová, A Zahoranová, D Kováčik, M Stupavská and M Černák. Polylactic acid surface activation by atmospheric pressure dielectric barrier discharge plasma. *Open Chemistry* 2015; **13**, 564-569.

[38] Z Krtouš, L Hanyková, I Krakovský, D Nikitin, P Pleskunov, O Kylián, J Sedlaříková and J Kousal. Structure of plasma (re)polymerized polylactic acid films fabricated by plasma-assisted vapour thermal deposition. *Materials* 2021; **14(2)**, 459.

[39] M Zarei, S Sayedain, A Askarinya, M Sabbaghi and R Alizadeh. Improving physio-mechanical and biological properties of 3D-printed PLA scaffolds via in-situ argon cold plasma treatment. *Scientific Reports* 2023; **13**, 14120.

[40] M Hanwell, D Curtis, D Lonie, T Vandermeersch, E Zurek and G Hutchison. Avogadro: An advanced semantic chemical editor, visualization, and analysis platform. *Journal of Cheminformatics* 2012; **4**, 17.

[41] W Mortier, S Ghosh and S Shankar. Electronegativity-equalization method for the calculation of atomic charges in molecules. *Journal of the American Chemical Society* 1986; **108**, 4315-4320.